STATICS PERFORMANCE EVALUATING AND OPTIMAL DESIGN OF A PARALLEL MECHANICAL LEG OF THE WHEEL-LEG HYBRID QUADRUPED ROBOT

Mengke Qu[1,2,3], Hongbo Wang[1,3,*] and Yu Rong[2]

[1]Parallel Robot and Mechatronic System Laboratory of Hebei Province
[3]Laboratory of Advanced Forging & Stamping Technology and Science of Ministry of Education
Yanshan University
No. 438, West Hebei Ave., Qinhuangdao 066004, P. R. China
410533309@qq.com; *Corresponding author: hongbo_w@ysu.edu.cn

[2]College of Urban Construction
Hebei Normal University of Science and Technology
No. 360, West Hebei Ave., Qinhuangdao 066004, P. R. China
lixiangcg@126.com

ABSTRACT. *A new type of wheel-leg hybrid quadruped robot is proposed, and it has four 6-DOF mechanical legs based on the 3-UPS parallel mechanism. The statics performance analysis and optimal design of the mechanical leg are done. First, using the vector chain method, the transmission model of the 3-UPS parallel mechanism is established, and the statics transmission equation is established. Also, a set of statics performance evaluation indexes is defined, and the statics performance of the leg mechanism is analyzed. Then, based on the statics performance evaluation indexes, the optimal design of structural parameters is done by Monte Carlo method. By establishing the probability space model of each structure parameter, an excellent set of structural parameters is found. Finally, using dynamic simulation software, the statics simulation analysis of the mechanical leg is done. These prove that the statics analysis and the structural parameters of the mechanical leg are very reasonable.*
Keywords: Wheel-leg hybrid robot, Parallel mechanical leg, Statics analysis, Performance evaluation index, Optimal design

1. **Introduction.** The wheel-leg hybrid quadruped robot has the advantages of both wheeled robot and legged robot. The common wheeled hybrid robot usually uses three configurations: first, Rolling-Wolf robot which is used for interstellar exploration [1]; second, wheel-leg hybrid robot with powered wheel mounted at the end of the mechanical leg [2]; third, the robot can skate with unpowered wheel mounted at the end of the mechanical leg [3]. If the wheeled mobile, step walking and skating skiing can be implemented on one robot, the robot's adaptability of ground pass will be greatly enhanced. Parallel mechanisms can achieve high speed and high acceleration movement, and their structures are compact [4]. Therefore, the parallel mechanisms are suitable for the mechanical legs of wheel-leg hybrid quadruped robot. The existing parallel mechanical legs mainly include: the WL-16 robot of Waseda University, Para-walker robot and NINJA robot of Tokyo Institute of Technology, elephant robot and octopus robot of Shanghai Jiao Tong University. Static analysis is very important to the robot's structure design [5-11]. Static analysis can avoid the stress concentration in the process of structural design. In this paper, a new kind of wheel-leg hybrid quadruped robot and its mechanical leg are proposed. The static modeling and static bearing capacity evaluation of the mechanical leg are carried out by using the vector loop method. Structural parameters optimization design of the

mechanical leg is done by Monte Carlo method. An excellent set of structural parameters is found.

2. **Wheel-Leg Hybrid Quadruped Robot and Parallel Mechanical Leg.** The wheel-leg hybrid quadruped robot is shown in Figures 1(a) and 1(b). It is composed of one trunk and four 6-DOF mechanical legs. It can move by wheeled mobile, step walking and skating skiing in different environments.

The parallel mechanical leg is shown in Figure 1(c), and its mechanism prototype is 3-UPS parallel mechanism. Here, the letter U is on behalf of universal joint; the letter P is on behalf of prismatic joint; the letter S is on behalf of spherical joint. The 3-UPS parallel mechanism has a fixed platform, a moving platform, and three UPS branches. One end of each UPS branch is connected to the fixed platform through universal joint, and the other end is connected to the foot platform through spherical joint. Therefore, the fixed platform has three joint points, and the layout of the three points is an isosceles right triangle. Based on screw theory [11], the moving platform of 3-UPS parallel mechanism has 6 DOF. The 3 moving joints of each branch are selected as driving joints, and the 3 revolute joints which are close to the fixed platform of each universal joint are selected as driving joints too.
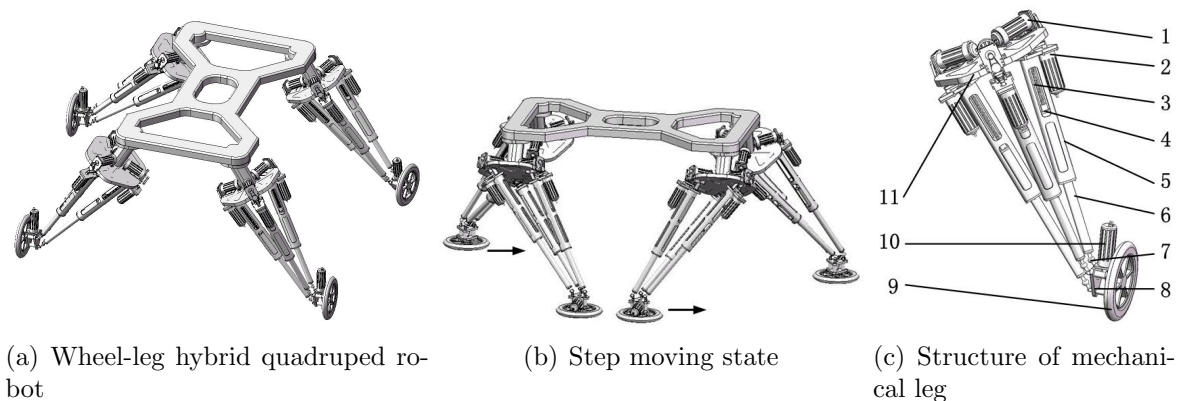
(a) Wheel-leg hybrid quadruped robot (b) Step moving state (c) Structure of mechanical leg

1. Servo motor, 2. Servo motor part, 3. Screw, 4. Nut, 5. Sleeve, 6. Rod
7. Spherical joint, 8. Foot, 9. Wheel, 10. Wheel motor, 11. Fixed platform

FIGURE 1. Structure of the robot and mechanical leg

3. **Kinematics Modeling of the Mechanical Leg.**

3.1. **Coordinate system definition and attitude description.** The vector diagrams of 3-UPS parallel mechanism are shown in Figure 2. In order to facilitate modeling, A_i $(i = 1, 2, 3)$ represents center of universal joint which connected to the fixed platform; B_i $(i = 1, 2, 3)$ represents center of spherical joint which connected to the moving platform; A_1 and B_1 are placed at the right angle vertex points of the isosceles right triangles. Define structural parameters of fixed platform $A_1A_2 = A_1A_3 = a$ and structural parameters of moving platform $B_1B_2 = B_1B_3 = b$; define the length of each branch $A_iB_i = l_i$ $(i = 1, 2, 3)$. $A_1 - x_1y_1z_1$ is defined as the global coordinate frame of the mechanism, x_1 axis and the A_1 universal joint's rotation axis which is close to the fixed platform are coincidence, z_1 axis is perpendicular to the plane of $A_1A_2A_3$, and the direction of y_1 axis is in line with the right-hand rule. $A_i - x_iy_iz_i$ $(i = 2, 3)$ is defined as the auxiliary coordinate frame, x_i axis and the A_i universal joint's rotation axis which is close to the fixed platform are coincidence, z_i axis is parallel to z_1 axis, and the direction of y_i axis is in line with the right-hand rule. $B_1 - upw$ is defined as the moving platform's local coordinate frame, w axis is perpendicular to the plane of $B_1B_2B_3$, u axis and the line B_1B_2 are coincidence,
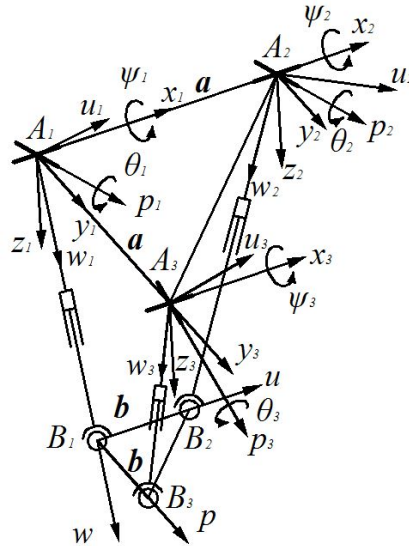
FIGURE 2. Sketch map of mechanical leg's 3-UPS mechanism

and p axis is in line with the right-hand rule. In order to describe the attitude of each branch, $A_i - u_i p_i w_i$ $(i = 1, 2, 3)$ is defined as the local coordinate frame of each branch, w_i axis and the line $A_i B_i$ are coincidence, p_i axis and the A_i universal joint's rotation axis which is far away from the fixed platform are coincidence, and u_i axis is in line with the right-hand rule. So, the attitude of each branch's local coordinate frame $A_i - u_i p_i w_i$ $(i = 1, 2, 3)$ relative to coordinate frame $A_i - x_i y_i z_i$ $(i = 1, 2, 3)$ can be obtained through 2 rotations: first, rotate ψ_i degrees around the x_i axis; second, rotate θ_i degrees around the p_i axis. The initial position of the moving platform is defined as: the moving platform is parallel to the fixed platform, and the distance between the two platforms is located in the middle of the total variation range h.

In order to facilitate the analysis, define primary structure parameters: $a = 230$ mm, $b = 70$ mm, $l_i \in (550, 950)$ mm $(i = 1, 2, 3)$, $h = 750$ mm. The rotation matrix of the local coordinate $A_i - u_i p_i w_i$ $(i = 1, 2, 3)$ is constructed:

$$\boldsymbol{R}_i = \text{Rot}\,(x_i, \psi_i)\,\text{Rot}\,(p_i, \theta_i) = \begin{bmatrix} \boldsymbol{u}_i & \boldsymbol{p}_i & \boldsymbol{w}_i \end{bmatrix}, \quad (i = 1, 2, 3) \tag{1}$$

where $\boldsymbol{u}_i$, $\boldsymbol{p}_i$ and $\boldsymbol{w}_i$ are the unit principal vectors of u_i, p_i and w_i in $A_1 - x_1 y_1 z_1$.

So, ψ_i $(i = 1, 2, 3)$ is the drive input angle of each universal joint's motor. B_1 is selected as the reference point of the moving platform. The attitude description of moving coordinate $B_1 - upw$ in $A_1 - x_1 y_1 z_1$ is:

$$\boldsymbol{R} = \text{Rot}\,(z_1, \beta)\,\text{Rot}\,(y_1, \beta)\,\text{Rot}\,(x_1, \gamma) = \begin{bmatrix} \boldsymbol{u} & \boldsymbol{p} & \boldsymbol{w} \end{bmatrix} \tag{2}$$

where $\boldsymbol{u}$, $\boldsymbol{p}$ and $\boldsymbol{w}$ are the unit principal vectors of u, p and w in $A_1 - x_1 y_1 z_1$.

3.2. **The solution of Jacobi matrix.** The closed loop vector constraint equation is established in $A_1 - x_1 y_1 z_1$:

$$\boldsymbol{l}_1 = l_1 \boldsymbol{w}_1 \tag{3}$$

$$\boldsymbol{l}_1 = \boldsymbol{a}_i + l_i \boldsymbol{w}_i - \boldsymbol{b}_i, \quad (i = 2, 3) \tag{4}$$

where l_i and $\boldsymbol{w}_i$ $(i = 1, 2, 3)$ are the length and unit principal vector of branch i, $\boldsymbol{a}_2$ is the vector of $A_1 A_2$, $\boldsymbol{a}_3$ is the vector of $A_1 A_3$, $\boldsymbol{b}_2$ is the vector of $B_1 B_2$, and $\boldsymbol{b}_3$ is the vector of $B_1 B_3$.

By solving derivative of Formulas (3) and (4), we can obtain:

$$\boldsymbol{v} = \dot{l}_1 \boldsymbol{w}_1 + l_1 \boldsymbol{\omega}_1 \times \boldsymbol{w}_1 \tag{5}$$

$$\boldsymbol{v} = \dot{l}_i \boldsymbol{w}_i + l_i \boldsymbol{\omega}_i \times \boldsymbol{w}_i - \boldsymbol{\omega} \times \boldsymbol{b}_i, \quad (i = 2, 3) \tag{6}$$

where $\boldsymbol{v}$ is the linear velocity of B_1, $\boldsymbol{\omega}$ is the angular velocity vector of moving platform, $\boldsymbol{\omega}_i$ and $\dot{l}_i$ are the angular velocity and the moving joint's velocity of branch i $(i = 1, 2, 3)$.

According to vector operations, $\boldsymbol{w}_i \cdot (\boldsymbol{\omega}_i \times \boldsymbol{w}_i) = 0$, $(i = 1, 2, 3)$. So, by doing dot product $\boldsymbol{w}_1$ on both sides of Formula (5), and doing dot product $\boldsymbol{w}_i$ $(i = 2, 3)$ on both sides of Formula (6), we can obtain:

$$\dot{l}_1 = \boldsymbol{w}_1^{\mathrm{T}} \boldsymbol{v} \tag{7}$$

$$\boldsymbol{w}_i^{\mathrm{T}} \boldsymbol{v} = \dot{l}_i - (\boldsymbol{b}_i \times \boldsymbol{w}_i)^{\mathrm{T}} \boldsymbol{\omega}, \quad (i = 2, 3) \tag{8}$$

By writing Formulas (7) and (8) in matrix form, we can obtain the relational model between $\boldsymbol{\dot{l}} = \begin{bmatrix} \dot{l}_1 & \dot{l}_2 & \dot{l}_3 \end{bmatrix}^{\mathrm{T}}$ and $\boldsymbol{V} = [\boldsymbol{v}^{\mathrm{T}} \ \boldsymbol{\omega}^{\mathrm{T}}]^{\mathrm{T}}$:

$$\begin{bmatrix} \dot{l}_1 \\ \dot{l}_2 \\ \dot{l}_3 \end{bmatrix} = \begin{bmatrix} \boldsymbol{w}_1^{\mathrm{T}} & 0 \\ \boldsymbol{w}_2^{\mathrm{T}} & (\boldsymbol{b}_2 \times \boldsymbol{w}_2)^{\mathrm{T}} \\ \boldsymbol{w}_3^{\mathrm{T}} & (\boldsymbol{b}_3 \times \boldsymbol{w}_3)^{\mathrm{T}} \end{bmatrix} \begin{bmatrix} \boldsymbol{v} \\ \boldsymbol{\omega} \end{bmatrix} \tag{9}$$

By writing Formula (9) in vector:

$$\boldsymbol{\dot{l}} = \boldsymbol{J}_1 \begin{bmatrix} \boldsymbol{v}^{\mathrm{T}} & \boldsymbol{\omega}^{\mathrm{T}} \end{bmatrix}^{\mathrm{T}} \tag{10}$$

where $\boldsymbol{\dot{l}} = \begin{bmatrix} \dot{l}_1 & \dot{l}_2 & \dot{l}_3 \end{bmatrix}^{\mathrm{T}}$ is the input velocity of moving joints, $\boldsymbol{J}_1$ is the mobile driven Jacobi matrix, $\boldsymbol{J}_1 \in \boldsymbol{R}^{3 \times 6}$.

According to angular velocity superposition principle, we can obtain:

$$\boldsymbol{\omega}_i = \dot{\psi}_i \boldsymbol{x}_i + \dot{\theta}_i \boldsymbol{p}_i, \quad (i = 1, 2, 3) \tag{11}$$

where $\boldsymbol{\omega}_i$ is the overall angular velocity of branch i $(i = 1, 2, 3)$, $\boldsymbol{x}_i$ and $\boldsymbol{p}_i$ are the unit principal vectors of x_i and p_i in $A_1 - x_1 y_1 z_1$.

According to vector operations, $\boldsymbol{p}_i \times \boldsymbol{p}_i = 0$, $(i = 1, 2, 3)$. So, by doing cross product $\boldsymbol{p}_i$ $(i = 1, 2, 3)$ on both sides of Formula (11), we can obtain:

$$\boldsymbol{p}_i \times \boldsymbol{\omega}_i = \dot{\psi}_i (\boldsymbol{p}_i \times \boldsymbol{x}_i), \quad (i = 1, 2, 3) \tag{12}$$

According to vector operations, $\boldsymbol{p}_i \times \boldsymbol{w}_i = 0$, $(i = 1, 2, 3)$. So, by doing dot product $\boldsymbol{p}_1$ on both sides of Formula (5), and doing dot product $\boldsymbol{p}_i$ on both sides of Formula (6), we can obtain:

$$\boldsymbol{p}_1^{\mathrm{T}} \boldsymbol{v} = l_1 \boldsymbol{w}_1^{\mathrm{T}} (\boldsymbol{p}_1 \times \boldsymbol{\omega}_1) \tag{13}$$

$$\boldsymbol{p}_i^{\mathrm{T}} \boldsymbol{v} = l_i \boldsymbol{w}_i^{\mathrm{T}} (\boldsymbol{p}_i \times \boldsymbol{\omega}_i) - (\boldsymbol{b}_i \times \boldsymbol{p}_i)^{\mathrm{T}} \boldsymbol{\omega}, \quad (i = 2, 3) \tag{14}$$

By putting $\boldsymbol{p}_i \times \boldsymbol{\omega}_i$ $(i = 1, 2, 3)$ into Formulas (13) and (14), we can obtain:

$$\boldsymbol{p}_1^{\mathrm{T}} \boldsymbol{v} = \dot{\psi}_1 l_1 \boldsymbol{w}_1^{\mathrm{T}} (\boldsymbol{p}_1 \times \boldsymbol{x}_1) \tag{15}$$

$$\boldsymbol{p}_i^{\mathrm{T}} \boldsymbol{v} = \dot{\psi}_i l_i \boldsymbol{w}_i^{\mathrm{T}} (\boldsymbol{p}_i \times \boldsymbol{x}_i) - (\boldsymbol{b}_i \times \boldsymbol{p}_i)^{\mathrm{T}} \boldsymbol{\omega}, \quad (i = 2, 3) \tag{16}$$

By writing Formulas (15) and (16) in matrix form, we can obtain the relational model between $\boldsymbol{\dot{\psi}} = \begin{bmatrix} \dot{\psi}_1 & \dot{\psi}_2 & \dot{\psi}_3 \end{bmatrix}^{\mathrm{T}}$ and $\boldsymbol{V} = \begin{bmatrix} \boldsymbol{v}^{\mathrm{T}} & \boldsymbol{\omega}^{\mathrm{T}} \end{bmatrix}^{\mathrm{T}}$:

$$\begin{bmatrix} \dot{\psi}_1 \\ \dot{\psi}_2 \\ \dot{\psi}_3 \end{bmatrix} = \begin{bmatrix} \dfrac{\boldsymbol{p}_1^{\mathrm{T}}}{l_1 \boldsymbol{w}_1^{\mathrm{T}} (\boldsymbol{p}_1 \times \boldsymbol{x}_1)} & 0 \\ \dfrac{\boldsymbol{p}_2^{\mathrm{T}}}{l_2 \boldsymbol{w}_2^{\mathrm{T}} (\boldsymbol{p}_2 \times \boldsymbol{x}_2)} & \dfrac{(\boldsymbol{b}_2 \times \boldsymbol{p}_2)^{\mathrm{T}}}{l_2 \boldsymbol{w}_2^{\mathrm{T}} (\boldsymbol{p}_2 \times \boldsymbol{x}_2)} \\ \dfrac{\boldsymbol{p}_3^{\mathrm{T}}}{l_3 \boldsymbol{w}_3^{\mathrm{T}} (\boldsymbol{p}_3 \times \boldsymbol{x}_3)} & \dfrac{(\boldsymbol{b}_3 \times \boldsymbol{p}_3)^{\mathrm{T}}}{l_3 \boldsymbol{w}_3^{\mathrm{T}} (\boldsymbol{p}_3 \times \boldsymbol{x}_3)} \end{bmatrix} \begin{bmatrix} \boldsymbol{v} \\ \boldsymbol{\omega} \end{bmatrix} \tag{17}$$

By writing Formula (17) in vector:

$$\boldsymbol{\dot{\psi}} = \boldsymbol{J}_2 \begin{bmatrix} \boldsymbol{v}^{\mathrm{T}} & \boldsymbol{\omega}^{\mathrm{T}} \end{bmatrix}^{\mathrm{T}} \tag{18}$$

where $\dot{\boldsymbol{\psi}} = \begin{bmatrix} \dot{\psi}_1 & \dot{\psi}_2 & \dot{\psi}_3 \end{bmatrix}^{\mathrm{T}}$ is the input angular velocity of universal joints, $\boldsymbol{J}_2$ is the rotary driven Jacobi matrix, $\boldsymbol{J}_2 \in \boldsymbol{R}^{3\times 6}$.

By finishing Formulas (10)-(18), the velocity mapping relation of 3-UPS mechanism can be obtained.

$$\dot{\boldsymbol{q}} = \boldsymbol{J}\boldsymbol{V} \tag{19}$$

where $\boldsymbol{J} = [\boldsymbol{J}_1 \quad \boldsymbol{J}_2]^{\mathrm{T}}$ is Jacobi matrix, $\boldsymbol{J} \in \boldsymbol{R}^{6\times 6}$, $\dot{\boldsymbol{q}} = \begin{bmatrix} \boldsymbol{i} & \dot{\psi} \end{bmatrix}^{\mathrm{T}}$ is input velocity vector, $\boldsymbol{V} = [\boldsymbol{v} \quad \boldsymbol{\omega}]^{\mathrm{T}}$ is generalized velocity vector of moving platform.

4. Static Performance Analysis of the Mechanical Leg.

4.1. **Static transfer equation.** The output generalized force vector of the moving platform is defined as $\boldsymbol{F} = \begin{bmatrix} \boldsymbol{F}^{\mathrm{T}} & \boldsymbol{M}^{\mathrm{T}} \end{bmatrix}^{\mathrm{T}}$, and the driving force of the driving joints is defined as $\boldsymbol{\tau} = \begin{bmatrix} \tau_1 & \tau_2 & \tau_3 & \tau_4 & \tau_5 & \tau_6 \end{bmatrix}^{\mathrm{T}}$. According to the principle of virtual work [11], the sum of the input virtual work of all driving motion joints of the mechanism is equal to the sum of the virtual work of the generalized force of the moving platform:

$$\boldsymbol{\tau}^{\mathrm{T}}\boldsymbol{i} = \boldsymbol{F}^{\mathrm{T}}\boldsymbol{V} \tag{20}$$

where $\boldsymbol{i}$ is the virtual displacement of driving motion joints, $\boldsymbol{V}$ is the virtual displacement of moving platform.

By putting Formula (19) into Formula (20), we can obtain the static transfer equilibrium equation of mechanical leg:

$$\boldsymbol{F} = \boldsymbol{G}\boldsymbol{\tau} \tag{21}$$

where $\boldsymbol{G} = \boldsymbol{J}^{\mathrm{T}}$ is the force Jacobi matrix, $\boldsymbol{G} \in \boldsymbol{R}^{6\times 6}$.

4.2. **Static performance evaluation.** In $\boldsymbol{G} = \begin{bmatrix} \boldsymbol{G}_F^{\mathrm{T}} & \boldsymbol{G}_M^{\mathrm{T}} \end{bmatrix}$, $\boldsymbol{G}_F^{\mathrm{T}}$ is the force transfer sub-matrix, $\boldsymbol{G}_M^{\mathrm{T}}$ is transfer sub-matrix, so:

$$\boldsymbol{F} = \begin{bmatrix} \boldsymbol{F}^{\mathrm{T}} & \boldsymbol{M}^{\mathrm{T}} \end{bmatrix} = \begin{bmatrix} \boldsymbol{G}_F^{\mathrm{T}} & \boldsymbol{G}_M^{\mathrm{T}} \end{bmatrix} \boldsymbol{\tau} \tag{22}$$

where $\boldsymbol{G}_F^{\mathrm{T}} \in \boldsymbol{R}^{3\times 6}$, $\boldsymbol{G}_M^{\mathrm{T}} \in \boldsymbol{R}^{3\times 6}$.

Norm of Formula (22), we can obtain:

$$\|\boldsymbol{F}\|^2 = \boldsymbol{\tau}^{\mathrm{T}}\boldsymbol{G}_F^{\mathrm{T}}\boldsymbol{G}_F\boldsymbol{\tau}; \quad \|\boldsymbol{M}\|^2 = \boldsymbol{\tau}^{\mathrm{T}}\boldsymbol{G}_M^{\mathrm{T}}\boldsymbol{G}_M\boldsymbol{\tau} \tag{23}$$

Assume that the input value is a unit vector, and put Lagrange operator into Formula (24)

$$\boldsymbol{L}_F = \boldsymbol{\tau}^{\mathrm{T}}\boldsymbol{G}_F^{\mathrm{T}}\boldsymbol{G}_F\boldsymbol{\tau} - \lambda_F\left(\boldsymbol{\tau}^{\mathrm{T}}\boldsymbol{\tau} - 1\right); \quad \boldsymbol{L}_M = \boldsymbol{\tau}^{\mathrm{T}}\boldsymbol{G}_M^{\mathrm{T}}\boldsymbol{G}_M\boldsymbol{\tau} - \lambda_M\left(\boldsymbol{\tau}^{\mathrm{T}}\boldsymbol{\tau} - 1\right) \tag{24}$$

The extreme values of $\boldsymbol{L}_F$ and $\boldsymbol{L}_M$ are:

$$\frac{\partial \boldsymbol{L}_F}{\partial \boldsymbol{\tau}} = 0 : \boldsymbol{G}_F^T\boldsymbol{G}_F\boldsymbol{\tau} - \lambda_F\boldsymbol{\tau} = 0; \quad \frac{\partial \boldsymbol{L}_M}{\partial \boldsymbol{\tau}} = 0 : \boldsymbol{G}_M^T\boldsymbol{G}_M\boldsymbol{\tau} - \lambda_M\boldsymbol{\tau} = 0 \tag{25}$$

where λ_F and λ_M are the characteristic values of $\boldsymbol{G}_F^{\mathrm{T}}\boldsymbol{G}_F$ and $\boldsymbol{G}_M^{\mathrm{T}}\boldsymbol{G}_M$.

The extreme values of moving platform's output force and torque are:

$$\begin{cases} \|\boldsymbol{F}\|_{\max} = \sqrt{\lambda_{F\max}}, & \|\boldsymbol{F}\|_{\min} = \sqrt{\lambda_{F\min}} \\ \|\boldsymbol{M}\|_{\max} = \sqrt{\lambda_{M\max}}, & \|\boldsymbol{M}\|_{\min} = \sqrt{\lambda_{M\min}} \end{cases} \tag{26}$$

where $\lambda_{F\max}$, $\lambda_{F\min}$, $\lambda_{M\max}$, $\lambda_{M\min}$ are maximum and minimum singular values of $\boldsymbol{G}_F$ and $\boldsymbol{G}_M$.

So, $\|\boldsymbol{F}\|_{\max}$, $\|\boldsymbol{F}\|_{\min}$, $\|\boldsymbol{M}\|_{\max}$, $\|\boldsymbol{M}\|_{\min}$ are the maximum and minimum output force and torque values of moving platform. Define a set of static performance evaluation indexes:

$$\eta_F = \|F\|_{\max}; \quad \eta_M = \|M\|_{\max} \tag{27}$$

If the values of η_F and η_M are larger, the statics performance of the mechanical leg will be better. By using the mathematical software MATLAB to calculate the evaluation

(a) Curved surface of μ_F (b) Curved surface of μ_M
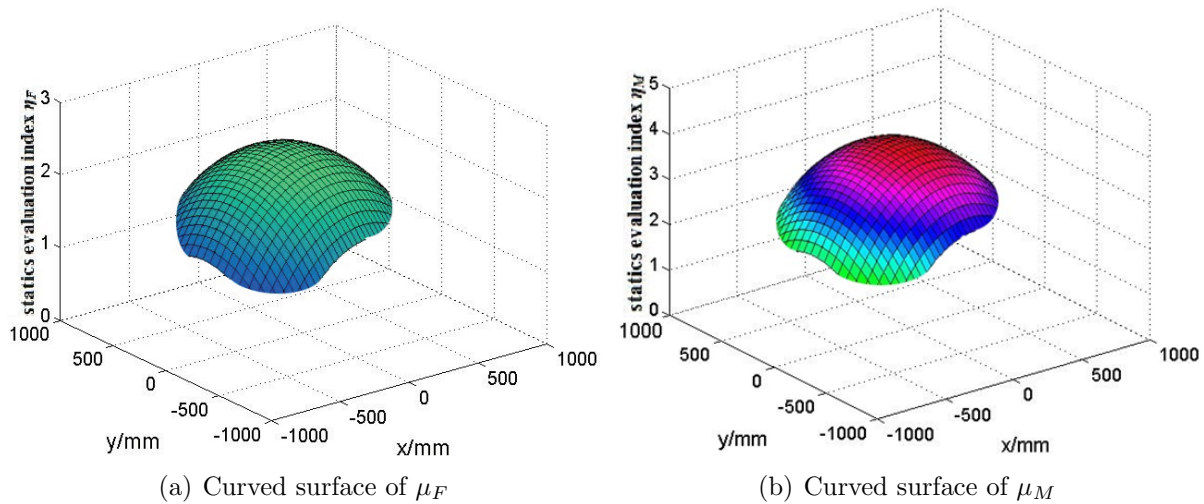
FIGURE 3. Distribution of static load carrying evaluation index

indexes of η_F and η_M, the distribution of static load carrying evaluation indexes in the workspace are shown in Figure 3.

Figure 3 shows, the static performance is better in the central area of the work space. We define another set of static performance evaluation indexes:

$$\bar{\eta}_F = \frac{\int_V \eta_F dV}{V}; \quad \bar{\eta}_M = \frac{\int_V \eta_M dV}{V} \tag{28}$$

where $\bar{\eta}_F$ and $\bar{\eta}_M$ are the global average values of η_F and η_M.

4.3. **Analysis of the relationship between static bearing capacity and structural parameters.** In order to find a set of structural parameters with good static performance, the relationship between the static bearing capacity and its structural parameters is analyzed. a and b are selected as the target object, and the value curves of η_F, η_M, $\bar{\eta}_F$, $\bar{\eta}_M$ are drawn shown in Figure 4.

Figure 4 shows, the values of η_F and $\bar{\eta}_F$ increase with the increase of a, the values of η_F and $\bar{\eta}_F$ decrease with the increase of b, η_M and $\bar{\eta}_M$ increase with the increase of a, η_M and $\bar{\eta}_M$ decrease with the increase of b.

5. Static Optimization and Simulation of Structural Parameters.

5.1. **Structural parameter optimization.** By using Monte Carlo method based on evaluation index, the range of the main structural parameters: $a \in (100, 350)$ mm, $b \in (20, 120)$ mm. By taking the intermediate value of each performance index as the probability model: $\eta_F = 1.8$, $\bar{\eta}_F = 1.9$, $\eta_M = 2.4$, $\bar{\eta}_M = 2.2$. Using the statistical probability function of MATLAB, the distributions of sampling values of each structural parameter are calculated shown in Figure 5.

By analyzing Figure 5, a set of structural parameter values considering various aspects of performance is determined given in Table 1.

5.2. **Static simulation.** In order to verify the rationality of structural parameters in Table 1, the Adams software is used to calculate the output forces of the moving platform when the different driving force/torque are input, and the simulation values are compared with the theoretical values given in Table 2.

Through the static loading in the simulation software, the simulation values are obtained as comparison value. So as Table 2 shows, the moving platform's output deviation generalized forces between the theoretical values and the simulation values are all less than 5 N; and the moving platform's output deviation generalized torques between the

(a) a and η_F, $\bar{\eta}_F$ curves

(b) b and η_F, $\bar{\eta}_F$ curves

(c) a and η_M, $\bar{\eta}_M$ curves

(d) b and η_M, $\bar{\eta}_M$ curves
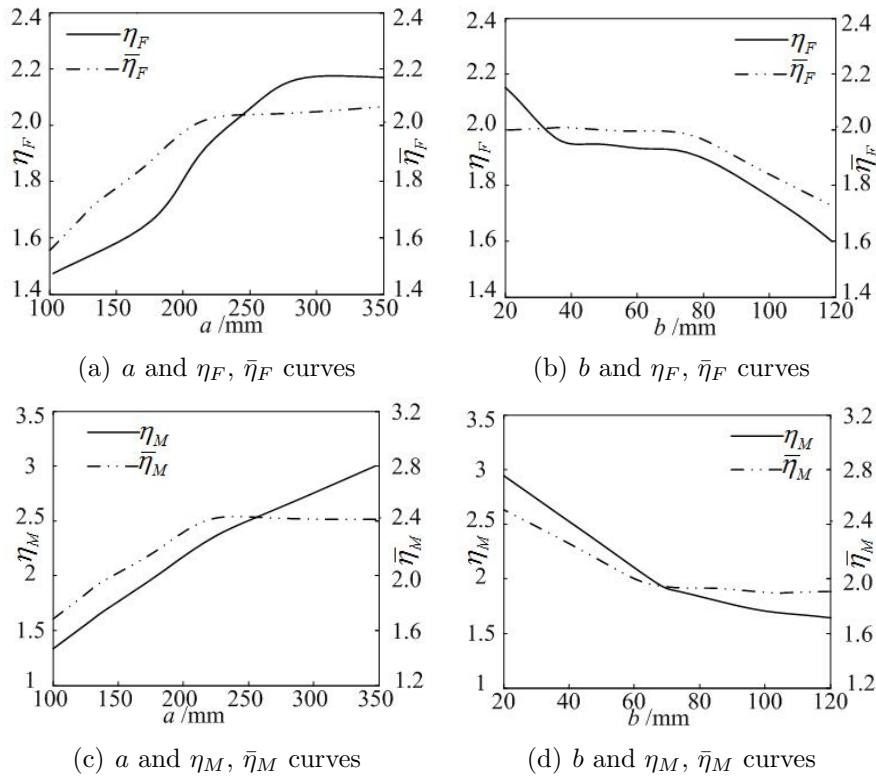
Note: a is the fixed platform's structure parameter, b is the moving platform's structure parameter, η_F, $\bar{\eta}_F$ and η_M, $\bar{\eta}_M$ are statics evaluation indexes.

FIGURE 4. Relationship curves of structure parameters and statics evaluation indexes η_F, $\bar{\eta}_F$, η_M, $\bar{\eta}_M$

(a) Parameter a probability graph

(b) Parameter b probability graph
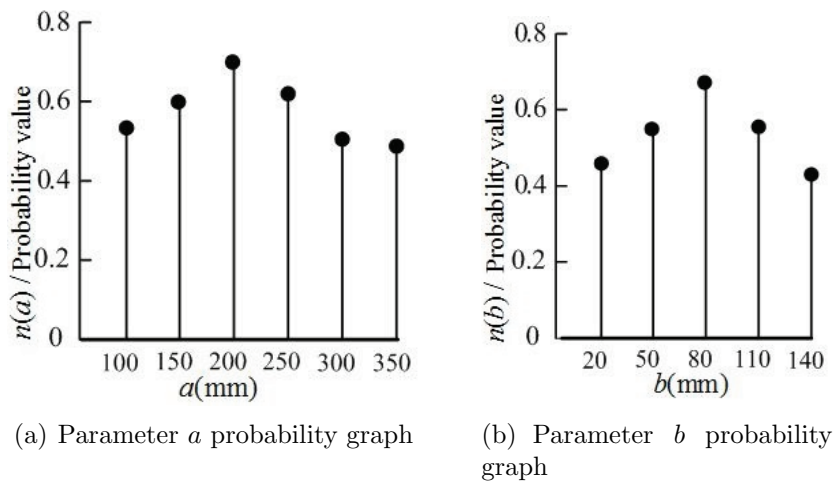
FIGURE 5. Probability distribution of structure parameters

TABLE 1. Structure parameters of mechanical leg (mm)

Name	Size/Model
structural parameter a of the fixed platform	200
structural parameter b of the moving platform	80
ball screw's length $\times$ diameter $\times$ wall thickness	$400 \times 10 \times 14$
cylinder's length $\times$ diameter $\times$ wall thickness	$500 \times 50 \times 5$
moving rod's length $\times$ diameter $\times$ wall thickness	$500 \times 30 \times 3$

TABLE 2. Comparison of simulation and theoretical statics data

	Driving force (N)	Driving torque (N·m)	Theoretical generalized force (N, N·m)	Simulation generalized force (N, N·m)
1	(130 110 120)	(0.6 0.7 0.7)	(271 137 313 0.13 0.15 0.11)	(265 308 309 0.11 0.13 0.10)
2	(130 120 130)	(0.6 0.5 0.7)	(243 118 287 0.17 0.13 0.15)	(238 115 283 0.14 0.10 0.13)
3	(110 130 120)	(0.7 0.8 0.6)	(257 143 297 0.15 0.11 0.13)	(253 138 293 0.13 0.10 0.11)
4	(110 120 110)	(0.5 0.7 0.8)	(261 133 286 0.18 0.17 0.16)	(257 130 281 0.15 0.16 0.13)
5	(120 130 120)	(0.7 0.5 0.6)	(277 123 307 0.16 0.13 0.12)	(272 118 301 0.13 0.11 0.11)
6	(120 110 110)	(0.8 0.7 0.6)	(231 112 273 0.13 0.11 0.14)	(227 109 270 0.11 0.10 0.13)
7	(130 120 120)	(0.8 0.5 0.7)	(281 143 309 0.17 0.16 0.18)	(279 137 303 0.14 0.15 0.16)
8	(130 110 110)	(0.8 0.6 0.7)	(277 136 298 0.16 0.14 0.15)	(273 132 294 0.15 0.12 0.13)

theoretical values and the simulation values are all less than 0.03 N·m. These results verify the correctness of the mechanical leg's static model established in this paper.

6. **Conclusions.**
(1) A wheel-leg hybrid quadruped robot and its 6-DOF parallel mechanical leg based on 3-UPS parallel mechanism are presented. The static transfer model of mechanical leg is established, and the distribution of the static bearing capacity evaluation index in the workspace is drawn based on the static model.

(2) Based on the static model, a set of static performance evaluation indexes is defined; the relationship between the structural parameters and the evaluation indexes of the static performance is analyzed. The influence of structural parameters on the static bearing capacity of mechanical legs is revealed.

(3) Considering the static performance evaluation index, Monte Carlo method is used to establish the probability model space of each structural parameter. Calculation shows, when the structural parameters are $a = 200$ mm, $b = 80$ mm, the mechanical load of the mechanical leg is the best. Based on the structural parameters, the static simulation analysis of the mechanical leg shows, the force/torque values of the mechanical leg's different output generalized forces are within a reasonable range.

(4) On the basis of static analysis of parallel mechanical leg, the prototype of the mechanical leg will be manufactured. Then, the walking test of the wheel-leg hybrid quadruped robot will be carried out.

REFERENCES

[1] R. Volpe, J. Balaram and T. Ohm, Rocky 7: A next generation Mars rover prototype, *Advanced Robotics*, vol.11, no.4, pp.341-358, 2016.
[2] C. Collins, Stiffness modeling and force distribution for the all-terrain hex-limbed extra-terrestrial explorer (ATHLETE), *ASME 2007 International Design Engineering Technical Conferences & Computers and Information in Engineering Conference*, Las Vegas, USA, pp.1-9, 2007.
[3] S. Hirose and G. Endo, Study on roller-walker (multi-mode steering control and self-contained locomotion), *Proc. of IEEE International Conference on Robotics and Automation*, no.3, pp.2808-2813, 2016.
[4] F. Gao and W. Z. Guo, Thinking of the development strategy of robots in China, *Chinese Journal of Mechanical Engineering*, vol.52, no.7, pp.1-6, 2016.
[5] J. Manyika, M. Chui and J. Bughin, *Disruptive Technologies: Advances that will Transform Life, Business, and the Global Economy*, McKinsey Global Institute, San Francisco, CA, USA, 2013.

[6] T. Zhang, Q. Li, C. S. Zhang et al., Current trends in the development of intelligent unmanned autonomous systems, *Frontiers of Information Technology & Electronic Engineering*, vol.18, no.1, pp.68-85, 2017.

[7] X. Zheng, Q. H. Liu, Y. J. Wu et al., Motion monitoring and analysis of Chang'E-3 rover based on same-beam VLBI differential phase delay, *Sci. Sin-Phys. Mech. Astron.*, vol.44, no.8, pp.872-878, 2014.

[8] Q. H. Liu, Y. J. Wu, Y. Huang et al., Mars rover positioning technology based on same-beam VLBI, *Sci. Sin-Phys. Mech. Astron.*, vol.45, no.9, 2015.

[9] L. W. Tsai, *Robot Analysis: The Mechanics of Serial and Parallel Manipulators*, John Wiley and Sons, New York, 1999.

[10] S. Joshi and L. W. Tsai, Jacobian analysis of limited-DOF parallel manipulators, *ASME Journal of Mechanical Design*, no.124, pp.254-258, 2002.

[11] Z. Huang, Y. S. Zhao and T. S. Zhao, *Advanced Spatial Mechanism*, Higher Education Press, Beijing, 2006 (in Chinese).